Enhanced and New Possible Functionalities of ATI-SAR through Multibaseline Acquisition and Modern Spectral Estimation Techniques

Fabrizio Lombardini, Federica Bordoni, Fulvio Gini
Dept. of "Ingegneria della Informazione", University of Pisa, via Diotisalvi 2, 56126 Pisa, Italy
Tel.: +39-(0)50-568511; Fax: +39-(0)50-568522; E-mail: {f.lombardini,f.bordoni,f.gini}@iet.unipi.it

***Abstract* - A brief discussion of some open problems of the conventional single-baseline along-track interferometric (ATI) technique for ocean sensing is given. A survey of previous research on advanced multibaseline ATI concepts is presented, stressing how multibaseline acquisition coupled with proper processing has great potential for improving the performance of ATI. Extended operation in critical conditions, reliable velocity extraction, enhanced imaging resolution and sensitivity can be obtained. In particular, a robust multibaseline velocity estimation technique is presented. It exploits the multibaseline Doppler resolution capability to produce estimates of ocean surface velocity that are robust to possible bimodal spectra of speckle, arising when both advancing and receding Bragg waves contribute to radar scattering. Bias and inflated variance for unexpected dual Bragg components in conventional ATI are analyzed. Three methods are proposed to process multibaseline data for robust estimation, based on Fourier transform, on adaptive Capon's filtering, or on super-resolution MUSIC spectral estimation. Performance is analyzed in detail by both simulation and the statistical Cramér-Rao bounding technique. Results show that this multibaseline technique may be effective to produce accurate estimates in absence of detailed local wind information. A vision of integration with other advanced ATI techniques is finally hinted.**

I. INTRODUCTION

Along-track SAR interferometry (ATI-SAR) is a promising technique for ocean remote sensing introduced by Goldstein and Zebker in 1987, when the concept was proposed and proved exploiting the NASA-JPL AIRSAR L-band platform [Gol87]. The original ATI technique uses a two-antenna SAR system, where the along-track baseline between the two elements of the interferometer produces a short time lag τ between the two complex SAR images formed by the returns received at each antenna. Estimation of the phase difference between the two images allows the mean short-term Doppler shift of the scattering from the ocean surface to be measured on a pixel by pixel basis [Tho93]. After compensating for the velocity of the radar-wavelength resonant Bragg waves, that are responsible of the scattering itself, the net radial surface velocity results, which is composed of translational motions and long (resolved) wave orbital motions [Tho93]. In principle such a system can also measure the scatterer ensemble coherence time, which depends, e.g., on speckle decorrelation due to modulation by medium (non-resolved) waves. Therefore, ATI systems have the potential to measure ocean surface currents, wind waves, internal waves, tidal water flows, sea wave-height spectra, and other surface dynamical features, at large scale and with high spatial resolution (see e.g. [Gol87], [Tho93], [She93], [Car94]).

This interferometric SAR technique for oceanic applications is relatively new and has not a full visibility in the oceanographic community, yet. To contribute to its spreading, a special session on interferometric applications over the ocean has been organized in the 2001 IEEE International Geoscience and Remote Sensing Symposium. It is currently recognized that ATI is capable of producing much richer information than classical intensity SAR imaging. The former technique is evolving rapidly, but it is not yet in a mature (fully operational) status. Some open problems still limit its potential performance. Also, some possible novel functionalities may be conceived that have not been investigated yet. Interestingly, the basic technique of ATI recently began evolving in the direction of multibaseline ATI, where more than two phase centers displaced along-the-track are employed [Orw92], [Car94], [Fri98], [Lom98], [Bar00]. A K two-way phase center uniform array with overall baseline B is employed, which acquires K complex SAR images at K–1 time-lags $\{l\tau/(K-1)\}_{l=1}^{K-1}$, being τ the overall time lag.

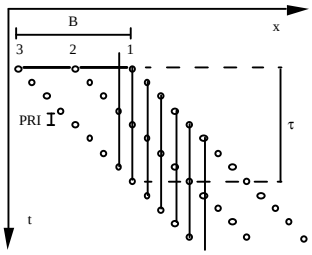

Fig. 1. Dual baseline ATI-SAR.

Fig. 1 shows the space-time location of the phase centers for K=3. From the three synthetic apertures, three SAR images of the same area can be obtained in identical geometry and with time lags $\tau/2$ and τ. The array of K two-way phase centers can be obtained by using K antennas with a doubled overall baseline, with one transmit/receive antennas and the other antennas qualified only on reception. As an alternative, for K=3 one can resort to transmitter ping-ponging between

This work has been supported by the Italian National Research Council (CNR).

just two antennas, effectively synthetizing three different equispaced two-way phase centers (see the AIRSAR system case [Car94]). Potentials of the multibaseline technique are discussed here.

The paper briefly overviews some of the problems of conventional ATI, and stress the possibility of getting enhanced performance by resorting to advanced multibaseline concepts. A short collection of pertinent references, which is very representative but by no means exhaustive, is commented. Also, it is shown how multibaseline ATI acquisition may be exploited not only for improving the operation of some of the existing ATI functionalities, but also to develop new possible useful functionalities. In particular, the robust multibaseline concept proposed in [Lom01] for operation in absence of detailed local wind information is developed and analyzed in detail. Finally, additional visions are hinted. In the authors' intention, this may contribute to stimulate the growing research interest in multibaseline ATI systems, models, and processing techniques, whose great potential in the direction of an accurate, flexibile and rich along-track interferometric sensing has still to be fully exploited.

II. Open Problems

The current problems of ATI that are briefly commented in this paper are the following:

1) Data noise.
2) Data inversion, and ancillary data.
3) Data blurring.

The problem of data noise 1) concerns accuracy of the radar parameter estimates (Doppler shift, coherence time), Doppler ambiguity, and system flexibility to varying operating conditions such as scene signal to noise ratio and ocean coherence time. Dealing with the problem of data noise means to enhance the existing ATI functionalities (i.e. retrieval of Doppler and coherence time maps). Multibaseline ATI is a way to cure the problem of data noise, exploiting baseline diversity and proper signal processing for data fusion. This is discussed in Sect. III. However, it is worth noting that the very potential of multibaseline ATI is to furnish additional functionalities for ATI sensing, that can be related to the solution of the other two problems of the conventional technique, as will be discussed in Sect. IV and V.

One is the problem of data inversion and ancillary data 2). This basic problem of conventional ATI regards the extraction of maps of physical parameters, such as ocean current velocities, from the maps of estimated radar parameters. In fact, there are conditions in which the interpretation of the radar parameters is ambiguous, e.g. when both advancing and receding Bragg waves are present in the resolution cell in close to crosswind condition. Usually this ambiguity is controlled resorting to in-situ ancillary data, such as local surface wind speed and direction. This can prevent ATI to be a flexible and fully autonomous remote sensing technique.

Another problem is that of data blurring 3). The dynamic of the ocean surface during the aperture synthesis produces well-known problems of defocusing and possible non-linear blurring in SAR images, and hence in ATI maps as well. ATI Doppler and coherence time maps are generally distorted, and maps obtained by post-processing of the radar parameter maps, such as sea waveheight spectra, can be distorted as well.

There are indications in recent literature that most of problems in 1), 2) and 3) may be mitigated or solved by means of advanced multibaseline ATI techniques. These possible solutions are referenced and commented in the following. Large space will be allowed in particular for new results obtained by the authors in the framework of problem 2), data inversion for surface velocity.

III. Reduction of Data Noise

An existing functionality of ATI is estimation of the ocean coherence time, which gives important information of roughness and turbulence phenomena [Car94]. As an example, surface wind speed and direction, and breaking waves affect the ocean coherence time. Although single-baseline interferometry is in principle enough for estimating ocean coherence time from interferometric coherence, accuracy cannot be good when coherence time is low or if ancillary data on coherence loss from thermal noise, which has to be compensated for, are not gathered [Car94]. Also, estimation of ocean coherence time from the one-lag correlation coefficient is based on an assumed autocorrelation model of backscatter, which may change according to the presence of a single or both the Bragg components, especially at L- and C-band. A single-baseline estimate may not distinguish between a single low-correlated component and two highly-correlated components whose superposition produces the same low single-lag coherence.

The other existing functionality of ATI is estimation of surface velocity. However, even when the necessary compensation for the velocity of the radar-wavelength resonant Bragg waves is perfect, estimation accuracy may not be satisfactory in critical conditions. These are low coherence time, e.g. from rough sea, or low signal-to-noise ratio from smooth surfaces [Car94]. The baseline length of conventional ATI, governing the time lag between the two SAR images, is usually chosen as a trade-off between interferometric phase sensitivity and speckle decorrelation, to minimise the variance of the Doppler estimate [Car94]. Performance in terms of Doppler unambiguous range is also taken into account. Although a single fixed baseline can reasonably trade-off among all these goals, it cannot stay optimal for highly varying ocean coherence time.

A. Multibaseline Estimation of Coherence Time

The ocean coherence time can be estimated more reliably if multiple along-track baselines are available, which allows to produce samples of the backscatter autocorrelation function with multiple time lags. This makes its parameters identifiable unambiguously and with low statistical errors.

In [Orw92] this principle is experimented by resorting to autoregressive (AR) spectral estimation [Sto97]. Another method is proposed and experimented in [Car94], where two coherence estimates for the K=3 (dual baseline) AIRSAR system are fused together. In these papers, neither assumptions on the presence of one or two Bragg components, nor derivation details are given. To fully exploit the time lag diversity, in [Bes00] a maximum likelihood (ML) ocean coherence time estimator has been proposed for a generic multibaseline system. The derivation is carried out for the single Bragg component assumption. ML estimation guarantees asymptotical (large number of looks N) statistical efficiency [Kay93], so that the proposed method can be considered the optimal processor. Simulated estimation accuracy is enhanced compared to single baseline interferometry, especially for low coherence time conditions [Bes00].

B. Multibaseline Estimation of Doppler Shift

In [Lom98] it is shown that proper fusion of multibaseline data can produce benefits for along-track interferometry in terms of both increased Doppler estimation accuracy, system flexibility to varying ocean coherence time, and possibly increased unambiguous Doppler range (see also [Car94]).

Again, a ML multibaseline Doppler estimator has been developed under the single Bragg component assumption, that optimally accounts for the presence of the multiplicative complex speckle noise effect corrupting the useful signal [Lom98], [Bes00]. Simulated estimation accuracy reveals that interesting gains in terms of minimum operating coherence time and signal-to-noise ratio can be achieved. It is worth recalling that the complexity and possible cost of multibaseline ATI systems can be relatively high, in terms of hardware, data storage, room for antennas (or number of platforms and weight for possible spaceborne formation-based implementations). Therefore, it is very important to extract information (Doppler shift and coherence time) with the highest possible quality, fully exploiting the multibaseline data content. This may make sophisticated ML processing, which is a parametric (model-based) spectral estimator, more desirable than simple suboptimal interferogram fusion methods, or Fourier-based multibaseline processors. A comparison of various multibaseline methods, carried out in the parallel area of cross-track interferometry, can be found in [Lom01b].

IV. Robust Data Inversion

For a reliable inversion of current velocities from Doppler maps, accurate ancillary data of local surface wind speed and direction are necessary to evaluate a reference spectrum of speckle, determined by short (Bragg) wind waves [Tho93]. Currents are then estimated from the advection of the estimated Doppler centroid compared to that of the reference spectrum [Rom00]. The reference spectrum can be bimodal when both advancing and receding Bragg waves are present in the resolution cell, for a geometry close to cross-wind. Conventional ATI, that only measures the Doppler centroid, can produce highly biased estimates of surface currents, if the wind direction and speed is not a-priori known and accurate compensation for the phase velocities of the two Bragg wave components is not possible [Tho93], [Mol98], [Rom00]. In fact, an unexpected power split ratio between the two possible Bragg components results in an unmodeled shift of the Doppler centroid. This inversion problem is particularly important for close to cross-wind geometry, low wind speed, and low radar carrier frequency (e.g. L- or C-band). As an alternative to resorting to auxiliary measurements or sensors, or in-situ ancillary data, the radar wavelenght and incidence angle may be optimized to minimize sensitivity to the non-unimodal spectrum scenario [Rom00].

It is worth noting that the dual Bragg component situation can affect also the variance of estimated surface velocity, which is generally inflated compared to the classical single Bragg component condition [Lom01]. In fact, it is expected that estimated Doppler shift by conventional ATI is erratic between the two Doppler peaks. This can be regarded as anomalous phase noise from low overall ocean coherence time, and can affect both measuring of currents and the retrieval of sea wave-height spectra, whose noise floor is raised.

In this paper the possibility is carefully investigated of exploiting multibaseline acquisition to produce estimates of ocean surface velocity that are intrinsically robust to possible bimodal spectrum situations, as hinted in [Tho93]. To this purpose, a concept has been proposed in [Lom01], which relies on the advanced multibaseline functionality of resolution in the Doppler shift domain, coming from the richer time sampling of backscatter than conventional ATI [Fri98], [Bar00], [Bes00]. The robust estimation concept is further developed here. This may constitute a step towards the development of the new possible functionality of autonomous operation of ATI.

A. Multibaseline Robust Velocity Estimation

The idea pursued in this paper is to exploit multibaseline Doppler resolution to solve the above mentioned inversion problem by a two-step procedure: i) *resolve* the two spectral peaks of the bimodal spectrum, and then ii) *identify* unambiguously the spectrum advection by current (or orbital

velocity). This is possible assuming an ambient -no surface velocity- spectrum whose peaks locations correspond to the advancing and receding Bragg frequency. This model is valid for low wind speed and high incidence angle, especially for low carrier frequency (L-, C-band) [Tho93]. The Doppler centroid measured by conventional ATI cannot distinguish between advection of the spectrum and centroid movement because of an unexpected second Bragg spectral component, while proper multibaseline spectrum resolution and identification can result in velocity estimates that are not hampered by a varying signal power ratio between the two Bragg components.

B. Statistical Data Model

The data model assumed in this study is an extension of the statistical multibaseline ATI data model in [Lom98], [Bes00]. A dual component signal is considered modeling the SAR-processed echo from the two Bragg components. Each component is affected by circular Gaussian distributed multiplicative noise with Gaussian shaped autocorrelation function [Lom98], [Rom00]. The multiplicative noise models the partially correlated speckle arising from the modulation by medium waves. Consider a *K*-phase center ATI system with overall time lag τ. The complex amplitudes of the pixels, corresponding to a same given patch of sea, observed in the *K* SAR images are arranged in the vector $\mathbf{y}(n) = [y_1(n) \cdots y_K(n)]^T$, for *n*= 1,2,…,*N*. *N* is the number of independent and identically distributed looks [Car94] available for the *K*-dimensional complex pixel vector. Each vector is modeled as

$$\mathbf{y}(n) = \mathbf{A}(\omega_1)\mathbf{x}_1(n) + \mathbf{A}(\omega_2)\mathbf{x}_2(n) + \mathbf{v}(n) \quad (1)$$

where $\mathbf{A}(\omega)$ is the steering matrix $\mathbf{A}(\omega) = diag\{1, e^{-j\omega\tau/(K-1)}, \cdots, e^{-j\omega\tau}\}$. ω_i are the mean Doppler shifts of the backscattered signal from the advancing (*i*=1) and receding (*i*=2) Bragg components considered separately. They are related to spectrum advection ω_a by $\omega_1 = \omega_a + \omega_B$, $\omega_2 = \omega_a - \omega_B$, respectively, where ω_B is the characteristic Bragg frequency. Vector $\mathbf{x}_i(n)$ represents the corresponding complex speckle term, with normalized coherence time $\tilde{\tau}_c = \tau_c / \tau$. Note that here we refer to the coherence time of each Bragg component considered in isolation, not to the conventional overall ocean coherence time. $\mathbf{v}(n)$ is complex white Gaussian thermal noise. As in [Tho93], [Bes00], this model does not take into account azimuth blurring from velocity bunching [She93].

C. Spectral and Advection Estimators

To estimate the Doppler spectrum, three methods are employed in this work. The first method is a) *Fourier*-based, being a multilook extension of the periodogram referred to as *Beamforming* (since it is usually applied as a spatial method for direction of arrival estimation) [Sto97]. The second method is a b) *Capon*'s estimator, belonging to the class of adaptive (data-dependent) filterbank approaches and producing better resolution and lower sidelobes than Fourier-based methods [Sto97]. The third method is a c) *root-MUSIC* algorithm, which is a super-resolution spectral estimator [Sto97].

Doppler resolution better than the Fourier limit and reduction of the associated leakage problems [Sto97] are very important characteristics in multibaseline ATI spectral estimation, given the limited time span τ of the data and the low number *K* of available time samples (phase centers). Being the antenna spacing (time sampling) uniform, a Toeplitz covariance matrix estimate is employed for the first two methods. A forward-backward covariance matrix estimate is used for root-MUSIC [Sto97].

To identify the advection ω_a of the estimated spectrum, two different techniques are proposed and investigated. The first technique, that we term 1) the *dual peak method* (DP), estimates the location of the two spectral peaks corresponding to the two Bragg components by finding the two highest peaks in the estimated spectrum. Then, the two estimates are ordered modulo the unambiguous Doppler range, and the advection ω_a is estimated as the difference between the higher (anti-clockwise rightmost) estimate $\hat{\omega}_1$ and the known characteristic positive Bragg frequency ω_B [Tho93], [Car94]. In other words, this algorithm aims to *lock to* and compensate for the advancing Bragg component, independently from the relative strength of the receding Bragg component.

However, sometimes two peaks cannot be found in Capon's spectrum when the receding component is too dim or too strong, because of the leakage (masking) effect. The same problem may arise for Beamforming with *K*=3, when the two components are too close and of similar power. In such case, the DP technique returns a 'non-operative' flag. The second technique aims to cure this problem, and we term it 2) the *virtual peak method* (VP). When a second spectral peak cannot be resolved, the VP technique attempts to reconstruct it by exploiting the a-priori information on the Bragg frequency. The Bragg frequency ω_B is added to and subtracted from the estimated peak location, and the estimated spectrum is evaluated at these two candidates frequencies. The location of the second peak, which is masked in the estimated spectrum, is the candidate frequency with the highest estimated spectrum value. Advection is then estimated as in the DP method. When the root-MUSIC spectral estimator is adopted, which is not based on spectral peak-picking and can always produce two frequency estimates, advection is estimated analogously to DP. However, this method is always operative, as VP is.

It is worth noting that ML estimation theory could be applied to model (1) to get an estimator of ω_a which is optimal, at least asymptotically. This has not been carried out yet, since the derivation and practical implementation of the ML advection estimator for two Bragg components present is even more involved than the complex derivation of the algorithm in [Bes00] commented in Sect. III B.

D. Analytical and Simulated Results

Two case studies have been analyzed using representative parameters for the AIRSAR along-track system operating at L-band. In this platform, K=3 equispaced phase centers are available through transmitter ping-ponging between the two antennas, with time lags of about 50 and 100 ms [Car94]. For conventional interferometry with K=2 phase centers, the $\tau = 50$ ms time lag is usually employed, since it provides performance trade-off for varying coherence, and large unambiguos Doppler range. The first case study assumes a multibaseline system operating with an overall time lag $\tau = 50$ ms, and an intermediate lag of 25 ms. This case might be realized by halving the current physical baseline of AIRSAR, and is termed the *short* overall baseline case. The time lag of the conventional interferometer used for performance comparison is $\tau = 50$ ms, the same as the overall time lag. Assuming an off-nadir angle of about $60°$, the Bragg frequency is such that $\omega_B \tau = 3\pi/8$ rad. The second case study represents the current configuration of AIRSAR, assuming for the multibaseline system an overall time lag $\tau = 100$ ms, and an intermediate lag of 50 ms. This case is termed the *long* baseline case. The conventional interferometer used for performance comparison has still $\tau = 50$ ms, which is now half of the multibaseline overall time lag. In both the case studies, two conditions are assumed for the correlation time of a Bragg component considered in isolation. A favourable condition for L-band is represented by $\tau_c = 200$ ms [Tho93], [Car94], [Rom00] and is termed *high* coherence time case. A less favourable case is considered with $\tau_c = 100$ ms [Car94], [Rom00] and is termed *low* coherence time case.

The corresponding bias and variance of the estimated advection have been evaluated by Monte Carlo simulation (10,000 trials) for the Beamforming-DP, Capon-DP, Beamforming-VP, Capon-VP, and MUSIC techniques, using data model (1). Where not otherwise stated, we assumed a total signal-to-noise ratio $SNR_{tot} = 24$ dB and N=32 looks, which are also representative parameters for the AIRSAR system [Car94].

The bound on ultimate achievable performance for the estimation problem at hand has also been evaluated. It is given by the *Cramér-Rao lower bound* (CRLB) from information theory. It states the minimum achievable variance for any unbiased estimator of a parameter of a statistical data model, depending on the *Fisher information* content intrinsic in the data [Kay93]. The CRLB on the estimated advection $\hat{\omega}_a$ has been evaluated for data model (1), assuming the other (nuisance) signal parameters are unknown but for ω_B. This bound is the extension of the classical interferometric CRLB in [Rod92] to the case of multibaseline data and dual Bragg condition. It is used in the sequel to judge the statistical efficiency of the proposed estimators, and can also be exploited for analytical performance prediction and system optimization.

Multibaseline spectral estimates

An example of the true signal power spectral density (PSD), given by the Fourier Transform of the autocorrelation sequence of the signal in (1), is reported in Fig.2 for the short baseline, high coherence time case. It has been computed for no advection and hence $\omega_1 = -\omega_2 = \omega_B$, where $\omega_B \tau = 3\pi/8$ rad. The normalized coherence time is $\tilde{\tau}_c = \tau_c / \tau = 4$. For the first curve the power ratio between the receding and advancing Bragg component is ΔSNR=-60 dB, so PSD centroid "c1" coincides with the compensation reference ω_B used by conventional ATI when only the advancing component ω_1 is taken into account (upwind assumption). When an unexpected non-negligible receding Bragg component is also present with ΔSNR=-6 dB, the centroid moves to "c2", causing a bias of 18% of the Bragg frequency for the conventional advection estimate that compensates for "c1". A typical realization of the multibaseline-estimated PSD for ΔSNR=-6 dB is also reported in Fig.2, for overall baseline equal to the single baseline of conventional ATI (same $\tau = 50$ ms). It is apparent how Beamforming may fail to resolve the two components, as expected since their separation is $\omega_1 - \omega_2 = 2\omega_B < 2\pi(K-1)/(K\tau) = \Delta\omega_F$, which is the Fourier resolution limit. Moreover, it is worth noting that the Beamforming spectrum with K=3 exhibits a single sidelobe in the unambiguous Doppler range, which is an unusual situation in spectral estimation. Finally, as expected, Capon's spectrum exhibits better resolution.

The consequent operating problems for the DP technique are quantified in Fig. 3, where the probability of operation $P_{op.DP}$ is reported, defined as the probability of finding two peaks in the estimated spectrum. The curves marked "sh." refer to the short baseline case. Capon-DP is often operative for ΔSNR around 0 dB (crosswind geometry), while if the receding component is too dim or too strong compared to the other, two peaks can be rarely found because of the leakage effect. The behavior of Beamforming-DP is dual: it is often non operative for ΔSNR around 0 dB, when neither the two components can be resolved nor a sidelobe appears in the estimated spectrum. Conversely, it is always operative when the receding component is dim or strong. However, it has to be noted that in this case one of the two peaks found is just a

sidelobe, i.e. a fake frequency estimate. Fig.3 also reports $P_{op.DP}$ for operation with the long overall baseline ($\tau = 100$ ms, curves marked "lg."). This produces higher resolution, at the cost of increased signal decorrelation (halved normalized coherence time $\tilde{\tau}_c = \tau_c / \tau = 2$). Beamforming-DP is now often operative even when the two components are of similar power, and probability of operation for Capon-DP is enhanced.

Performance and Cramér-Rao bounds

In the following, bias and standard deviation (std) of conventional (K=2) and multibaseline estimators are analyzed for varying ΔSNR. The normalized bias for the conventional advection estimate under the upwind assumption, $(\omega_1 - \eta_{\hat{\omega}_1})/\omega_B$, with η the circular expectation, is reported in Fig.4 for short baseline and high coherence time. The bias limit value is twice the Bragg frequency when the receding component is dominating. Beamforming-DP generally exhibits worse bias than conventional ATI, and little advantage is produced by adopting the VP version. On the contrary, Capon-DP exhibits negligible bias for ΔSNR=-6 dB, and reduces the bias for ΔSNR=0 dB (wich equals the Bragg frequency) by about 10 times. It also performs reasonably well when the receding component begins to dominate. This is obtained at the cost of a performance loss compared to conventional ATI for low ΔSNR. A bias arises in this region since the method needs two significant components being present to identify the right one for locking. Capon-VP can even perform better than Capon-DP, further reducing both the bias for high ΔSNR and the performance loss compared to conventional ATI for reasonably low ΔSNR. Also, it has the important advantage of being always operative (conversely, probability of operation for Capon-DP is non-unitary, see Fig. 3). When the super-resolution spectral estimator root-MUSIC is employed, resulting bias can be worse than Capon-VP, but std is always better, see Fig.4 (right). For ΔSNR=0 dB, std of conventional ATI is inflated by about 7 times compared to the single Bragg component situation. This std is reduced by about 2 and 5 times by Capon-VP and root-MUSIC, respectively.

It is worth noting that in this cross-wind condition the total ocean coherence time is significantly lower than the single-component $\tau_c = 200$, this is why std of conventional ATI strongly degrades. Interestingly, it results that proper multibaseline processing can produce a std close to that of conventional ATI operating in up- or downwind, virtually compensating for the loss of total coherence time coming from the mixing of the two Bragg components. Summarizing, both root-MUSIC and Capon-VP are better than Capon-DP in terms of probability of operation, but MUSIC generally outperforms Capon-DP, while Capon-VP tradeoffs bias for variance. As expected, getting a low std for large $|\Delta SNR|$ proved to be quite difficult, because all methods rely on two significative components being present.

The case of low coherence time is analyzed in Fig.5, still for the short baseline configuration ($\tau = 50$ ms, $\tau_c = 100$ ms, normalized coherence time $\tilde{\tau}_c = 2$). The bias for K=2 practically does not change for changing coherence time, while the bias control capability of the multibaseline methods is degraded in part. However, the general rankings among all the methods, including conventional ATI, are unaltered. The advantage of using MUSIC instead of Capon-DP is slightly reduced. This can be attributed to the fact that the super-resolution MUSIC estimator is based on a line spectra data model, so an increasing model mismatch develops for lowering τ_c (increasing bandwidth of the two spectral components). Also, Capon-VP gets a worse trade-off between bias and variance than for high coherence time. Consequently, Capon-DP may be now the best choice, but for the non-unitary $P_{op.DP}$.

Performance for different number of looks and total signal-to-noise ratio is investigated in Fig.6 and compared with the CRLB, for $\Delta SNR = 0$ dB, high coherence time. Beamforming-based methods are not reported since they do not perform well in this condition. For varying N, bias of all the methods is almost unaltered, while as expected std decreases with increasing number of looks. The rankings among the methods does not change with N, but for Capon-DP and Capon-VP tending to coincide asymptotically (large N). MUSIC is the most statistically efficient method, being quite close to the CRLB. However, it seems that it does not achieve the bound asymptotically (for N=256, its std is still 28% higher than the CRLB). This may be attributed to the fact that it operates under model mismatch and a single component is used for locking, so part of the data information content is not exploited. For decreasing SNR_{tot}, the biases are only slightly changing, while std of all methods increases. Capon-VP abruptly departs from the CRLB around $SNR_{tot} = 15$ dB, this threshold effect may be attributed to the sensitivity of the virtual peak reconstruction to high levels of thermal noise. Capon-DP has lower std than MUSIC for low SNR_{tot}, but MUSIC is still superior concerning the bias.

Fig. 7 reports performance for the current configuration of AIRSAR, where the multibaseline system has an overall time lag $\tau = 100$ ms (long baseline). The case considered here is high coherence time ($\tau_c = 200$ ms, normalized coherence time $\tilde{\tau}_c = 2$). The reference conventional interferometer is assumed to operate still with $\tau = 50$ ms, as usual. Performance of Beamforming- and Capon-based methods is partly improved compared to the short baseline case (see Fig. 4), because of the higher resolution. This

comes jointly with the enhanced $P_{op.DP}$ as seen in Fig. 3. Conversely, the halved $\tilde{\tau}_c$ makes MUSIC partly degrade especially in terms of bias. As a result, one may now consider Beamforming-VP and Capon-VP as the best options. Note that despite some gains are obtained by adopting the long baseline, the range of ΔSNR for which reasonably low std is obtained is slightly shrinked compared to the short baseline case. Also, the CRLB for varying ΔSNR, reported in the figure, shows that there is still room for improvement of the statistical efficiency of the robust multibaseline technique.

It is now worth noting that all the results commented so far can be regarded under a different point of view. Performance of the robust multibaseline techniques can be compared with conventional ATI operating with estimates obtained under an assumption different from upwind (and downwind). Fig. 8 reports the normalized bias of conventional ATI resulting from operation under the cross-wind assumption (all the others parameters being as in Fig. 7). It simply equals the bias in Fig. 7 minus 1. The reported performance of Capon-VP and MUSIC are exactly the same as in Fig. 7. What is important is that the performance loss in terms of bias for low ΔSNR is no more present. The multibaseline methods always exhibit a performance gain compared to conventional ATI, when the crosswind assumption on which it relies is violated (ΔSNR departing from 0 dB) to a limited extent.

Finally, Fig. 9 confirms that multibaseline operation with the long overall baseline may not be necessarily the best system option, as already argued from Fig. 7. For the reported condition of low coherence time ($\tau_c = 100$ ms, normalized coherence time $\tilde{\tau}_c = 1$), std is lowered compared to the corresponding short baseline case for the Beamforming-based methods, but it partly increases for those Capon-based, and MUSIC. One may now consider Capon-DP as the best option, taking also account of its bias, but not of the non-unitary $P_{op.DP}$. Again, the range of ΔSNR for which reasonably low std is obtained is slightly reduced compared to the short baseline case. Also, in this range std is higher than for short baseline. This may be partly compensated by the higher $P_{op.DP}$.

Results show that none of the proposed methods is uniformly most efficient, so a choice should be considered for an assumed typical scenario. Alternatively, one may develop a hybrid technique by proper adaptive selection. Also, the proposed approach appears to be robust to deviations from any wind azimuthal assumption that is necessary for conventional ATI. However, at this stage of development, the method may be more suitable for operation close to cross-wind than to up- or down-wind geometry. After validation with real data, the technique may be employed alternatively to or jointly with carrier and incidence angle optimisation [Rom00], obtaining a better overall system design in presence of contrasting requirements.

V. Deblurring

It is well known that conventional intensity SAR images of the ocean surface are blurred and non-linearly distorted (velocity bunching). The process of aperture synthesis cannot distinguish phase histories arising from azimuth displacements from that originating from Doppler shifts, so the orbital velocities of long waves and Doppler spread from finite ocean coherence time produce misplacements of signal contribution in the image. In particular, the effective image resolution can be much worse than the nominal one [Car94]. Since blurring acts at the single-look complex SAR image level, also interferometric products (Doppler and coherence time maps) are blurred and distorted.

Interestingly, the Doppler resolution capability intrinsic in multibaseline along-track interferometry may be exploited also in this direction, producing another new functionality of along-track interferometry, that of deblurring.

A. Multibaseline Intensity Deblurring

In [Fri98] a multibaseline technique is proposed and simulated, which allows partially compensating for the blurring of the intensity image. Each scatterer is misplaced during synthetic aperture processing by an amount depending on its velocity. Therefore, pixel by pixel estimation of Doppler spectrum, by Fourier transforming along the position index of the multibaseline array (i.e., the image index), allows relocation of the misplaced energy contribution. A practical problem of this technique may be the high number of phase centers necessary to get good restoration of the image resolution (K=16 in the reported case study).

B. Multibaseline Deblurring of Complex Data

A possible extension of this technique has been hinted in [Bes00] for deblurring of every possible interferometric product. The simple concept is relocating each *complex* SAR image acquired by the multibaseline system, after this operation any possible interferometric processor, including all those discussed in Sect. III and IV, can be applied to the relocated complex data set. In other words, a proper multibaseline processor may be applied to deblur the multibaseline data set, and subsequently the accurate and/or robust multibaseline processors may operate on it, virtually free from blurring problems. The suggested Doppler-driven multibaseline deblurring of complex data involves both Doppler analysis and inverse Fourier transformation [Bes00]. The problem of the large K necessary to get an accurate pixel by pixel Doppler analysis might be lightened by resorting to adaptive spectral estimators such as Capon. Use of a

minimum redundant (non uniform) array might also be considered.

C. Multibaseline Doppler Filtering

Finally, it is worth mentioning another possible new application of multibaseline Doppler resolution capability in the context of enhancing image quality. In [Bar00], multibaseline Doppler filtering is proposed and experimented to filter out the effect of certain scattering mechanisms, so enhancing the visibility of others. This may be useful for cleaning what can be considered clutter for a given application, increasing imaging sensitivity to the desired physical mechanisms. This clutter removal procedure is somewhat related to some of the Doppler analysis concepts in [Fri98], but is applied to a minimal multibaseline configuration (K=3).

VI. Conclusions

A brief survey of previous research on multibaseline ATI techniques has been presented. Multibaseline acquisition coupled with proper processing has great potential for improving the performance of ATI, in terms of extended operating envelope in critical conditions, reliable velocity extraction, imaging resolution and quality. A robust multibaseline velocity estimation technique has been presented and analyzed in detail. Results show that the proposed approach constitutes an interesting step towards making ATI sensing flexible and possibly autonomous from ancillary information such as local surface wind speed and direction. Future work could investigate detection of the number of significant Bragg components to automatically start the robust estimation algorithm. Moreover, other modern spectral estimators can be applied. Other advection estimators can be also conceived, such as the mean of the two peak location estimates, not assuming known Bragg frequency, which is reasonable, e.g., for high sea states. This and other locking methods will be presented in [Bor02]. Finally, a possible synergy can be envisaged between robust multibaseline velocity estimation and vector-ATI concepts. Vector ATI can image the velocity vector in place of the single radial component, by acquiring multiple interferograms from different azimuthal viewing angles (see, e.g., [Ros00], [Mol02]). However, the possible bias on each radial measure may affect the velocity vector estimate, and bias control methods may be of help. On the other hand, the effectiveness of robust multibaseline velocity estimation depends on the azimuthal viewing geometry relative to wind, so that viewing angle diversity may be beneficial. Proper integration of the two techniques might result in very accurate and autonomous vector estimates.

References

[Bar00] Barber B., “Recent advances in ocean remote sensing using imaging radar,” *J. of Defence Science*, 5 (3), F50-F58, 2000.

[Bes00] Besson O., Gini F., Griffiths H.D., Lombardini F., “Estimating ocean surface velocity and coherence time using multichannel ATI-SAR systems,” *IEE Proc.–Part F*, 147 (6), pp. 299-308, Dec. 2000.

[Bor02] Bordoni F., Gini F., Lombardini F., Verrazzani L., “A class of algorithms for multibaseline ATI-SAR oceanic surface velocity estimation in presence of bimodal Doppler spectrum,” *to be presented at EUSAR 2002*, Cologne, Germany.

[Car94] Carande R.E., “Estimating ocean coherence time using dual-baseline interferometric synthetic aperture radar,” *IEEE Trans. on Geosci. and Remote Sensing*, 32 (4), pp. 846-854, July 1994.

[Fri98] Friedlander B., Porat B., “VSAR: a high-resolution radar system for ocean imaging,” *IEEE Trans. on Aerospace and Electronic Systems*, 34 (3), pp. 755-776, July 1998.

[Gol87] Goldstein R.M., Zebker H.A., “Interferometric radar measurement of ocean surface currents,” *Nature*, 328 (20), pp. 707-709, Aug. 1987.

[Kay93] Kay S.M., *Fundamentals of statistical signal processing, estimation theory*, New Jersey, Prentice Hall, 1993.

[Lom98] Lombardini F., Griffiths H.D., Gini F., “A ML multichannel ATI-SAR technique for measuring ocean surface velocities,” *Proc. IEEE Oceans'98 Conf.*, Nice, France, pp.778-782, Sept.-Oct. 1998.

[Lom01] Lombardini F., Gini F., Matteucci P., “Multibaseline ATI-SAR for robust ocean surface velocity estimation in presence of bimodal Doppler spectrum,” *Proc. IEEE IGARSS 2001*, Sydney, July 2001.

[Lom01b] Lombardini F., Griffiths H.D., “Optimum and suboptimum estimator performance for multibaseline InSAR,” *EUSAR 2000 Special Issue, Frequenz – Zeitschrift fuer Telekommunikation (Journal of Telecommunications)*, Schiele & Schoen, Berlin, 55, pp.114-118, March/April 2001.

[Mol98] Moller D., Frasier S.J., Porter D.L., McIntosh R.E., “Radar-derived interferometric surface currents and their relationship to subsurface current structure,” *J. Geophysical Res.*, C6, pp. 12839-12852, 1998.

[Mol02] Moller D., Pollard B., Rodriguez E., “Coastline monitoring from a spaceborne vector-ATI radar: a mission concept,” *this Workshop*.

[Orw92] Orwig L.P., Held D.N., "Interferometric ocean surface mapping and moving object relocation with a Norden Systems Ku-band SAR," *Proc. IEEE IGARSS'92*, Houston, TX, pp.1598-1600, May 1992.

[Rod92] Rodriguez E., Martin J.M., “Theory and design of interferometric synthetic aperture radars,” *IEE Proc.–Part F*, 139 (2), pp. 147-159, April 1992.

[Rom00] Romeiser R., Thompson D.R., “Numerical study on the along-track interferometric radar imaging mechanism of oceanic surface currents,” *IEEE Trans. on Geosci. and Remote Sensing*, 38 (1), pp. 446-458, Jan. 2000.

[Ros00] Rosen P.A., Hensley S., Joughin I.J., Li F.K., Madsen S.N., Rodriguez E., Goldstein R.M., “Synthetic aperture radar interferometry,” *Proc. of the IEEE*, 88 (3), pp. 331-382, March 2000.

[She93] Shemer L. *et al.*, “Estimates of currents in the nearshore ocean region using interferometric synthetic aperture radar,” *J. Geophysical Res.*, (C4), pp. 7001-7010, 1993.

[Sto97] Stoica P., Moses R., *Introduction to spectral analysis*, New Jersey, Prentice Hall, 1997.

[Tho93] Thompson D.R., Jensen J.R., “Synthetic aperture radar interferometry applied to ship-generated internal waves in the 1989 Loch Linnhe experiment,” *J. Geophysical Res.*, (C6), pp. 10259-10269, June 1993.

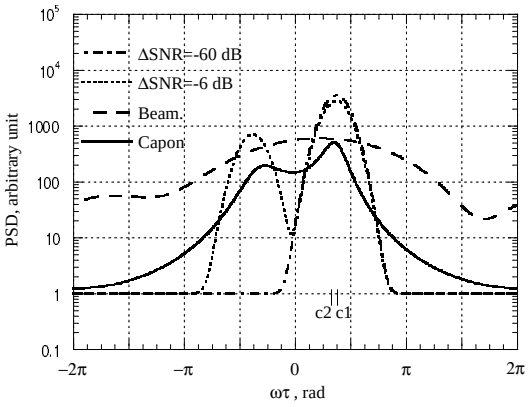

Fig. 2. True and estimated Doppler spectrum, short baseline, high coherence time.

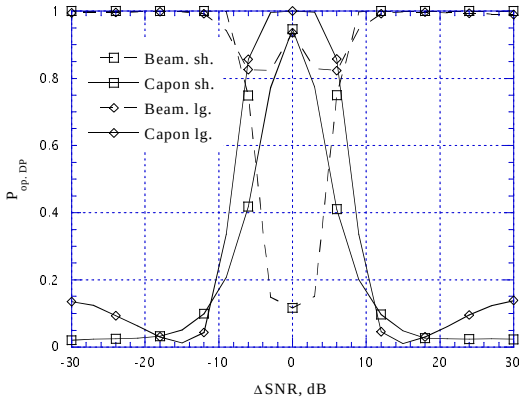

Fig. 3. Probability of operation for DP, short and long baseline, high coherence time.

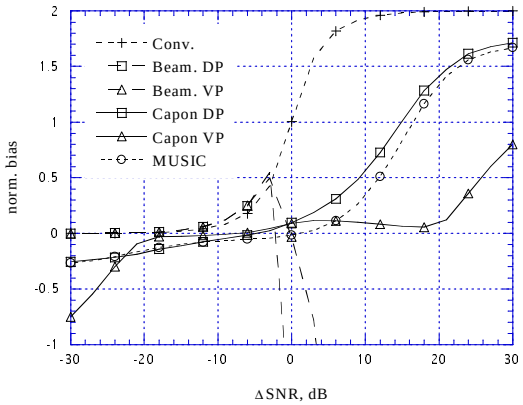

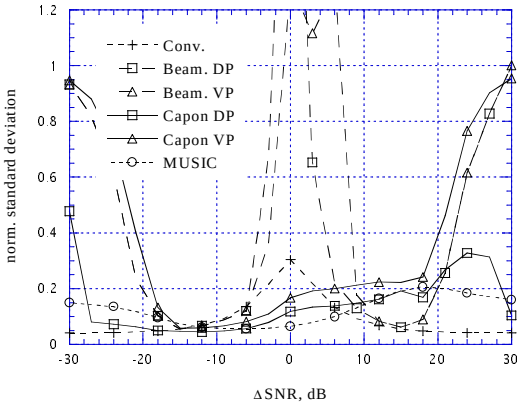

Fig. 4. Bias and std of estimated advection of Doppler spectrum, short baseline, high coherence time.

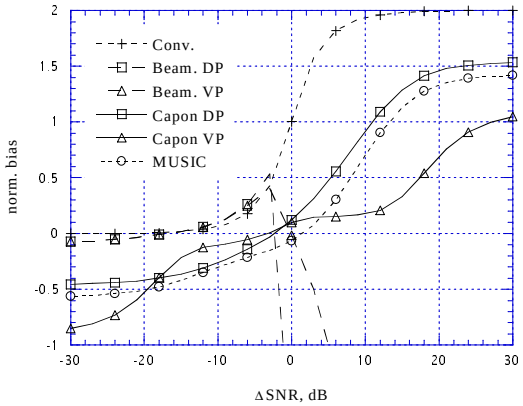

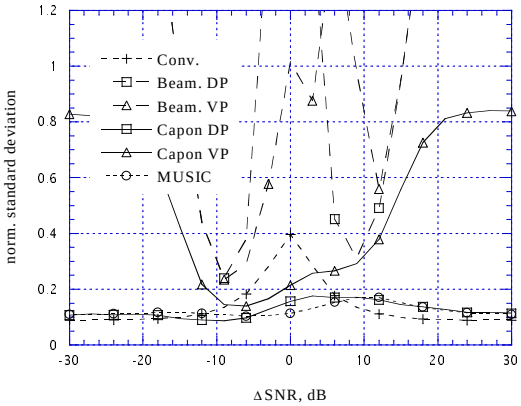

Fig. 5. Bias and std of estimated advection of Doppler spectrum, short baseline, low coherence time.

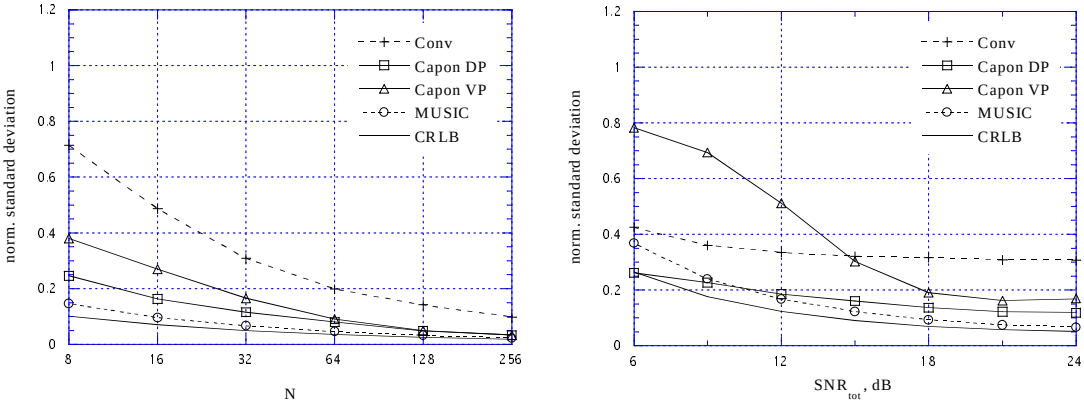

Fig. 6. Std of estimated advection of Doppler spectrum,
short baseline, high coherence time.

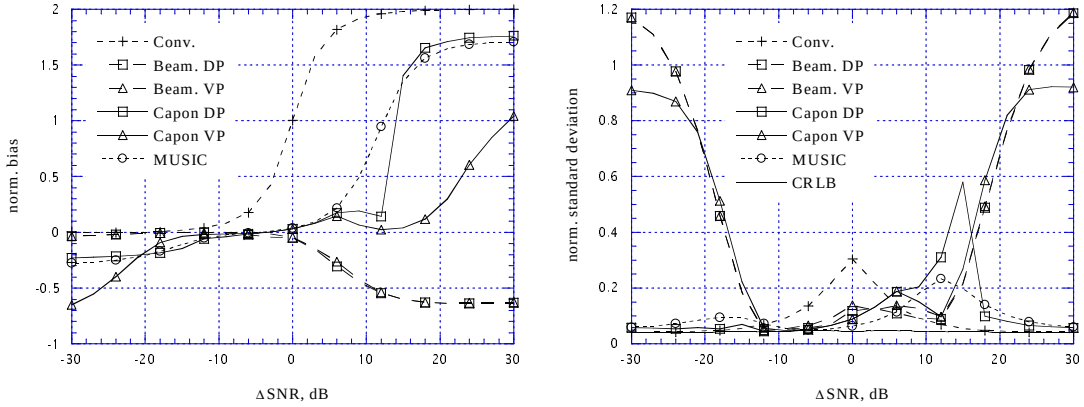

Fig. 7. Bias and std of estimated advection of Doppler spectrum,
long baseline, high coherence time.

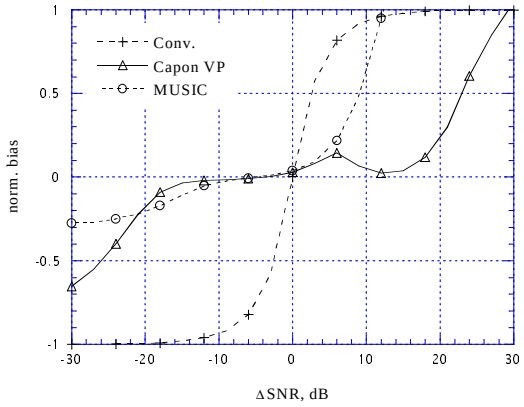

Fig. 8. Bias of estimated advection of Doppler spectrum,
long baseline, high coherence time, cross-wind assumption.

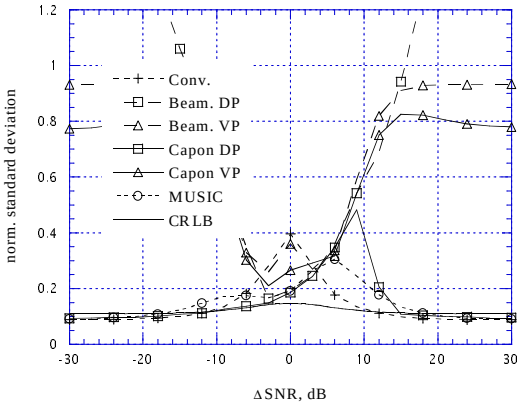

Fig. 9. Std of estimated advection of Doppler spectrum,
long baseline, low coherence time.